



# Characteristics of microbial denitrification under different aeration intensities: Performance, mechanism, and co-occurrence network

Haiguang Yuan<sup>a,b</sup>, Shaobin Huang<sup>a,b,c,\*</sup>, Jianqi Yuan<sup>a,b</sup>, Yingying You<sup>a,b</sup>, Yongqing Zhang<sup>a</sup>

<sup>a</sup> School of Environment and Energy, South China University of Technology, Higher Education Mega Center, Guangzhou 510006, PR China

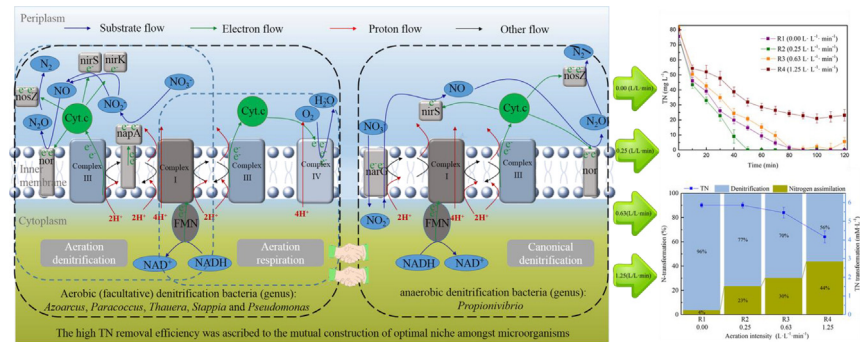
<sup>b</sup> Guangdong Ecological Environment Control Engineering Technology Research Center, South China University of Technology, Higher Education Mega Center, Guangzhou 510006, PR China

<sup>c</sup> State Key Laboratory of Pulp and Paper Engineering, Plant Micro/Nano Fiber Research Center, South China University of Technology, Guangzhou 510640, PR China

## HIGHLIGHTS

- TN and COD can be removed under aerobic condition within mixed bacteria consortia.
- Moderate aeration optimize NADH production and denitrification enzyme structure.
- Aeration reactors were dominated by facultative aerobic denitrifiers.
- High TN removal efficiency was ascribed to the mutual construction of optimal niche.

## GRAPHICAL ABSTRACT



## ARTICLE INFO

### Article history:

Received 8 July 2020

Received in revised form 9 August 2020

Accepted 23 August 2020

Available online 25 August 2020

Editor: Frederic Coulon

### Keywords:

Aerobic denitrification

Aeration intensity

NADH

Keystone taxa

Co-occurrence network

## ABSTRACT

This study aimed to explore how dissolved oxygen (DO) affected the characteristics and mechanisms of denitrification in mixed bacterial consortia. We analyzed denitrification efficiency, intracellular nicotinamide adenine dinucleotide (NADH), relative expression of functional genes, and potential co-occurrence network of microorganisms. Results showed that the total nitrogen (TN) removal rates at different aeration intensities (0.00, 0.25, 0.63, and 1.25 L/(L·min)) were 0.93, 1.45, 0.86, and 0.53 mg/(L·min), respectively, which were higher than previously reported values for pure culture. The optimal aeration intensity was 0.25 L/(L·min), at which the maximum NADH accumulation rate and highest relative abundance of *napA*, *nirK*, and *nosZ* were achieved. With increased aeration intensity, the amount of electron flux to nitrate decreased and nitrate assimilation increased. On one hand, nitrate reduction was primarily inhibited by oxygen through competition for electron donors of a certain single strain. On the other hand, oxygen was consumed rapidly by bacteria by stimulating carbon metabolism to create an optimal denitrification niche for denitrifying microorganisms. Denitrification was performed via inter-genus cooperation (competitive interactions and symbiotic relationships) between keystone taxa (*Azoarcus*, *Paracoccus*, *Thauera*, *Stappia*, and *Pseudomonas*) and other heterotrophic bacteria (OHB) in aeration reactors. However, in the non-aeration case, which was primarily carried out based on intra-genus syntrophy within genus *Propionivibrio*, the co-occurrence network constructed the optimal niche contributing to the high TN removal efficiency. Overall, this study enhanced our knowledge about the molecular ecological mechanisms of aerobic denitrification in mixed bacterial consortia and has theoretical guiding significance for further practical application.

© 2020 Elsevier B.V. All rights reserved.

\* Corresponding author at: School of Environment and Energy, South China University of Technology, Higher Education Mega Center, Guangzhou 510006, PR China.  
E-mail address: [chshuang@scut.edu.cn](mailto:chshuang@scut.edu.cn) (S. Huang).

## 1. Introduction

As a novel biological denitrification technology, the aerobic denitrification proposed by Robertson and Kuenen (1984) is attracting increased attention because TN can be simultaneously removed through chemical oxygen demand (COD) removal under an aerobic condition in a single reactor (Yang et al., 2020a; Zhang et al., 2019). To date, most studies have focused on single-strain identification and its application, and a large number of bacteria capable of aerobic denitrification have been isolated, including *Thiosphaera pantotropha*, *Alcaligenes faecalis*, *Pseudomonas putida* (Li et al., 2012), *Pseudomonas stutzeri* T13 (Feng et al., 2020), *Pseudomonas stutzeri* YZN-001, *Klebsiella pneumonia* CF-S9, and *Acinetobacter* sp. SYF26 (Du et al., 2017). Although pure strains have good removal efficiencies for specific pollutants, the ability of mixed bacterial consortia to resist external disturbances, maintain community stability, and degrade pollutants is better than that of pure culture. In the treatment of coal-based ethylene glycol industry wastewater by adding *Pseudomonas*, Du et al. (2017) found a decrease in nitrogen removal with decreased abundance of *Pseudomonas*. Zhang et al. (2019) performed a nitrogen removal research based on mixed-cultured consortia, including three highly active bacteria isolated from sediment by ultrasonic processing. They found that the mix culture has better nitrogen removal efficiency than the pure culture, especially in real wastewater application. Studies on the aerobic denitrification of mixed bacterial consortia are few (Yang et al., 2020b), and knowledge on the mechanism of aerobic nitrate reduction in activated sludge ecosystems remains largely insufficient. Thus, an important aspect that remains unclear is whether a much higher denitrification efficiency could be obtained in activated sludge (e.g., mixed bacterial consortia) with much more related functional microorganisms under aerobic conditions.

DO is the main factor affecting aerobic denitrification efficiency (Ji et al., 2015). Studies on pure culture aerobic denitrification have shown that the optimum specific growth rate and denitrification rate are achieved when the DO is 2–6 mg/L (Ji et al., 2015). However, in view of the influence of DO on aerobic denitrification under the condition of activated sludge, things are different. On one hand, Oh and Silverstein (1999) pointed out that the denitrification activity decreased to only 4% of that under the anoxic condition when the DO level is as high as 5.6 mg/L. On the other hand, Luo et al. (2014) proposed that no distinct difference exists between the nitrate or TN removal performance of low-oxygen and anoxic groups. Moreover, high-throughput sequencing analysis has indicated that compared with salinity, DO has no obvious influence on OOT numbers in marine reactors for nitrogen removal (Deng et al., 2017). Thus, under the condition of activated sludge, due to the interaction amongst different microorganisms or other factors, the effects of DO on denitrification efficiency differ from those under the condition of pure culture. Two mechanisms exist regarding oxygen effect on aerobic denitrification, as speculated by Gao et al. (2010). First is co-respiration, i.e., both nitrate and oxygen are used as electron acceptors simultaneously in a single strain. This mechanism indicates a competition for electrons within the electron-transport chain, resulting in enhanced denitrification upon oxygen depletion. Second is separate respiration, i.e., the nitrate respiration and oxygen respiration amongst microorganisms are separated, and denitrification is not kinetically inhibited by oxygen nor can oxygen compete for electrons. However, to the best of our knowledge, no consensus amongst researchers has been reached regarding the oxygen effect on aerobic denitrification in activated sludge.

As reported by an environmental microbiologist, denitrification and aerobic respiration depend on the same core respiratory machinery consisting of NADH dehydrogenase, quinone pool, and cytochrome *c* (Chen and Strous, 2013; Yang et al., 2020a). Meanwhile, the content of NADH depends on the kinetic balance between its production (by catabolism) and consumption (by denitrification, respiration, and anabolism) and is extremely sensitive to changes in cellular

electro-accepting mechanisms. According to a research by Wan et al. (2019), tetrabromobisphenol A can decrease the generation of NADH and eventually inhibit the denitrification activity. To explore the central carbon-flux pathways in nitrate reduction, Chen et al. (2020) found that NADH participates in the reduction of nitrate of *Paracoccus thiophilis* under aerobic condition and is regenerated through the TCA cycle, which is significantly affected by oxygen concentration. Accordingly, we speculated that any parameter controlling carbohydrate metabolism or electron production and consumption ultimately affects the denitrifying capability of denitrifiers.

We hypothesized that aerobic and anoxic denitrifiers are inextricable in pure culture and mixed bacterial consortia, however, as growth conditions in practical cases are highly variable and rarely optimal, nitrogen turnover by certain bacteria is bound to be inefficient. Yang et al. (2020b) applied metagenomics tools to study nitrogen removal in WWTPs and found that only five metagenomic assembled genomes can encode the entire denitrification pathway. Orellana's research on nitrogen removal from soil and activated sludge has also yielded similar results, i.e., none of their studied functional-group genomes can encode the complete denitrification pathway (Orellana et al., 2018). Thus, cooperation amongst microbial populations is the main contributor to nitrogen removal in wastewater treatment. For example, the synergistic effect of aerotolerant and heterotrophic bacteria is enhanced in solid-phase denitrification and the presence of oxygen probably stimulates denitrifier proliferation in a high-salinity reactor, thereby accelerating the reduction rate of nitrate (Deng et al., 2017). A network analysis has been conducted to investigate the co-occurrence and interactions of *Bacillus subtilis*, *Pseudomonas stutzeri*, and *Rhodococcus* sp. under aerobic denitrification and found that mixed bacterial consortia can realize 86% TN and 93% COD removal efficiency of real wastewater, respectively (Zhang et al., 2019). Synergistic effects of co-growth on denitrification and phosphorus removal have also been observed by Andersson et al. (2011), and these effects are affected by inter-species interactions with respect to biofilm formation, denitrification activity, and EPS composition. From a microbial metabolic and ecological point of view, in mixed bacterial consortia, the co-occurrence and network amongst key functional microorganisms has ecological (e.g., quorum sensing (Whiteley et al., 2017) and cheating effect (Leinweber et al., 2017)) and metabolic (e.g., obligate mutualistic metabolism including syntrophy, symbiotic relationship, and competitive interaction) functions (Morris et al., 2013).

Few studies have focused on the phenomenon of better TN removal in mixed bacterial consortia than that in pure culture. Accordingly, in the present study, we investigated for the first time the effects of aeration intensity on denitrifying performance in activated sludge through the distribution of NADH and the relative abundance of key denitrification genes. Then, the causes of aeration intensity shaping the microbial community of primary denitrifying bacteria were explored by assays of bacterial population. Finally, the microbial metabolic characteristics and potential networks were analyzed under different aeration intensities.

## 2. Materials and methods

### 2.1. Measurements, chemical reagents, and operation of experiments

Measurements were carried out with four identical continuous-aeration completely mixed batch reactors with different aeration intensities, namely, 0.0, 0.25, 0.63, and 1.25 L/(L·min) respectively. The corresponding mixed bacterial consortia were obtained from the reactors in this laboratory. These reactors were operated for more than 6 months under continuous-aeration operational mode and displayed stable aerobic denitrification performance. The synthetic denitrification medium contained the following (g/L): disodium succinate, 1.26; KNO<sub>3</sub>, 0.6 (NO<sub>3</sub><sup>-</sup>-N, 0.083); Na<sub>2</sub>HPO<sub>4</sub>·7H<sub>2</sub>O, 7.9; KH<sub>2</sub>PO<sub>4</sub>, 1.5; TP, 1.26; MgSO<sub>4</sub>·7H<sub>2</sub>O, 0.1; and 1 mL/L trace element solution based on a previous study (Sun Y. et al., 2019). Na<sub>2</sub>HPO<sub>4</sub>·7H<sub>2</sub>O, and

$\text{KH}_2\text{PO}_4$  were used to buffer the pH ( $7 \pm 0.1$ ) of the influent. The liquid volume-exchange ratio was 65%, and the biomass was maintained at 30% of the total working volume controlled by daily manual drainage to maintain the total biomass concentration of  $2112.27 \pm 300$  mg/L. Biomass concentration was assessed by protein analysis of small biomass samples as described by Guimerà et al. (2016) with modifications as shown in S1. A microporous aeration stone was placed at the bottom, and a magnetic agitation system was equipped at 110 rpm in each vessel. The working volume was 500 mL at a moderate temperature of ( $25 \pm 0.5$  °C) to overcome the insufficient aeration issues caused by hydraulics factors. In each measurement, samples were collected every 10 min and lasted for 2 h. Each time, 5 mL of mixed-liquor suspended solids was collected, of which 3 mL of supernatant was immediately filtered with a  $0.45 \mu\text{m}$  syringe and stored at 4 °C. Nitrogen-balance analysis was used to estimate the characteristics of carbon and nitrogen metabolism quantitatively (Huang et al., 2015; Zhang et al., 2019). TN without filtration was analyzed according to the method proposed by (Huang et al., 2015) using an ultrasonic cell disruptor (SCIENTZ-II D; Ningbo Scientz Biotechnology Co., Ltd., Ningbo, China). About 1 mL of precipitated activated sludge was used to analyze TN (inclusion of intracellular nitrogen). The intracellular nitrogen level was calculated by subtracting TN in supernatant from the TN value in precipitated activated sludge. Furthermore, 1 mL of precipitated activated sludge was used to analyze NADH content. When the experiment was carried out to 1 h, the activated-sludge samples collected from the four reactors and were denoted as R1 (0.0 L/(L·min)), R2 (0.25 L/(L·min)), R3 (0.63 L/(L·min)), and R4 (1.25 L/(L·min)). They were immediately treated with liquid nitrogen and stored at  $-80$  °C for bacterial qPCR assay and high-throughput sequencing. Each measurement was performed with at least three repetitions, and the results are presented as the mean  $\pm$  standard deviations. ANOVA was performed using SPSS software (SPSS Statistics version 19.0), and  $P_{0.05} > 0.05$  was considered as having no statistical significance.

## 2.2. Biochemical analysis methods

DO, pH, temperature, and concentrations of  $\text{NO}_3^-$ ,  $\text{NO}_2^-$ , and  $\text{NH}_4^+$  were measured following a previously established method (Sun C. et al., 2019). TN, COD were analyzed based on the standard method (APHA, 2005). Real-time liquid  $\text{N}_2\text{O}$  and NO concentrations were measured with an assorted microsensor multi-metre ( $\text{N}_2\text{O}$ -50 and NO-50, respectively; Unisense A/S, Aarhus, Denmark) according to previous research (Domingo-Félez et al., 2014) with some modifications, i.e., signals were logged using a picoammeter every 10 s. Within 1 week, intracellular NADH content was detected with a commercial Germs NADH Elisa Kit purchased from Quanzhou Ruixin Biological Technology Co., LTD (Fujian, China) according to the instructions. NADH content was calibrated with standard solutions of NADH, and the final NADH levels were calculated as per milligram of protein.

## 2.3. Bacterial qPCR assay

The key denitrification genes analyzed in this study and their primers are listed in (S2). qPCR was carried out in a 96-well plate with a total reaction volume of 20  $\mu\text{L}$  per well in the StepOne Plus PCR System (ABI, Foster, CA, USA) using a SYBR@Green qPCR Master mix (Hangzhou Biosci Co., Ltd., China). PCR was carried out under the following conditions: initial steps held at 95 °C for 3 min; and 45 cycles each of which including 95 °C with 5 s for melting and 60 °C with 30 s for annealing. Dissociation was carried out according to instrument guidelines. To achieve consistency of expression, considering its slight variability, 16S rRNA gene was used as the reference transcript for normalization between samples. qPCR data were obtained by mathematical calculation between the CT value of the internal reference gene and the

CT value of the gene to be tested, as well as by the relationship between the expression quantity differences amongst samples.

## 2.4. Bacterial analysis by using high-throughput sequencing

The genomic DNA of each sample was extracted using a MAG Bind Soil DNA kit (Omega Bio-tek, USA) and analyzed by agarose gel electrophoresis to evaluate the integrity of genomic DNA. Genomic DNA was accurately quantified using a Qubit3.0 DNA kit (Life Technologies, China) to determine the amount of DNA added in the PCR reaction. Primer 341F (CCCTACACGACGCTCTTCCGATCTG (barcode) CCTACGGGNGGCWGCAG) and primer 805R (GACTGGAGTTCCTTGGACCCGAGAA TTCCAGACTACHVGGGTATCTAATCC), encompassing the hypervariable V3–V4 region of the bacterial 16S rRNA gene, were prepared and the two PCR reactions procedure were performed based on a previous study (Xu et al., 2018). After PCR, the products were verified by agarose gel electrophoresis and purified with DNA clean beans. The purified product was quantified with a Qubit3.0 DNA kit (Life Technologies, China). After complete mixing, the PCR product was sequenced by Sangon Biotechnology, Co., Ltd. (Shanghai, China) using the Illumina MiSeq platform. The correlation coefficient and *P* value between communities was calculated using SparCC version 1.0.0 by selecting genus information with  $>1\%$  abundance. The potential interactions amongst microorganisms were analyzed by the way. PICRUSt 1.0.0 was used to analyze the primary functional differences amongst various samples.

## 2.5. Calculation of nitrate, substrate, and intermediate transformation efficiency

The removal efficiencies of  $\text{NO}_3^-$ , TN, and COD were calculated according to Eq. (1), in which  $[S]_{in}$  is the concentration of nitrate, TN, and COD in influent, and  $[S]_{out}$  is that in the effluent. The TN removal rate was calculated based on Eq. (2), in which  $\Delta t$  is the period between the sampling point. The NADH accumulation rate was calculated based on Eq. (3). The electron flux to nitrate was calculated according to Eq. (4), as described by a previous study with some modifications (Jia et al., 2019).

Nitrate, TN, and COD removal efficiency:

$$RE_S(100\%) = \frac{[S]_{in} - [S]_{out}}{[S]_{in}} \quad (1)$$

TN removal rate:

$$SRE_{TN}(100\%) = \frac{[TN]_{t1} - [TN]_{t0}}{[TN]_{t0} \times \Delta t} \quad (2)$$

NADH accumulation rate:

$$AE_{NADH}(100\%) = \frac{[NADH]_{t1} - [NADH]_{t0}}{[NADH]_{t0} \times \Delta t} \quad (3)$$

Electron to  $\text{NO}_3^-$ :

$$E_{Nitrate} = \frac{N_2}{14} \times 5 + \frac{N_2O}{14} \times 4 + \frac{NO}{14} \times 3 + \frac{NO_2^-}{14} \times 2 \quad (4)$$

## 3. Results and discussion

### 3.1. Denitrification performance of four reactors

#### 3.1.1. Determination of appropriate C/N ratio with different aeration intensities

As aforementioned, C/N ratio indicates the regulation of denitrification (Ji et al., 2015). Thus, the nitrate and TN removal efficiency under different aeration intensities and C/N ratio in 1 h were analyzed. As

shown in Fig. 1, the C/N ratio and aeration intensity affected TN removal efficiency, and denitrification efficiency increased with increased C/N ratio. At C/N = 4, 82.50% nitrate and 65.15% TN removal efficiencies were achieved even when the aeration intensity was 1.25 L/(L·min). At C/N = 6, 99.25% nitrate and 81.32% TN removal efficiencies were achieved. In general, C/N ratio is the main factor determining the denitrification efficiency of a system, and an increase in C/N ratio within a certain range can increase the denitrification efficiency by supplying electron donors (Peng et al., 2020). Notably, when the C/N ratio was 0, TN removal was also achieved to some extent, which may be related to the endogenous respiration of microbial bacteria. As reviewed by Ji et al. (2015), to satisfy the optimal growth and metabolic capacity requirements of aerobic denitrifiers, the optimal C/N load ratio was about 5 (sometimes 9–10), which was higher than that of canonical anoxic denitrification. Combined with the above conclusions, we selected C/N = 4.5 for subsequent investigations regarding the effects of different aeration intensities on aerobic denitrification.

### 3.1.2. Analysis of the distribution patterns of intermediates under different aeration intensities

Denitrification experiments with C/N = 4.5 were carried out, and the removal patterns of TN, COD,  $\text{NO}_3^-$ , and  $\text{NO}_2^-$  with time were obtained (Fig. 2). Results showed that at least 85.12%  $\text{NO}_3^-$  and 70.35% TN removal efficiency were achieved within 2 h at different aeration intensities, respectively. The TN removal rates in R1, R2, R3, and R4 were 0.93, 1.45, 0.86, and 0.53 mg/(L·min), respectively. To the best of our knowledge, these values were higher than the reported denitrification efficiency, especially the aerobic denitrification of pure culture (Table S2). This finding may be ascribed to the mutual construction of an optimal niche amongst microorganisms in a homogeneous system. Aeration can accelerate the degradation potency of COD in an aeration denitrification system compared with a non-aeration case, which could be related to the different ways of microbial assimilation under different oxygen concentrations. In other words, one (aeration systems) was primarily aerobic respiration, whereas the other was fermentation accompanied by nitrate respiration. In the multi-metabolism co-occurrence case, the switch from fermentative or nitrate respiration to aerobic respiration can realize redox balance and achieve optimal energy conservation through proton translocation linked to ATP synthesis (Feng et al., 2020). This finding may explain the higher TN removal rate in R2 than in R1 and the lower accumulation of nitrite in R2 than in R1. Furthermore, as proposed by Deng et al. (2020a, 2020b), TN removal rate could also be increased by the enhancement of carbon source on assimilation. As shown in Table 1, the TN removal rates in R1, R2, R3, and R4 were lower than the removal rates of nitrate. This observation

illustrated that dissimilatory nitrate reduction to nitrogen dominated the removal of nitrate, and that nitrate assimilation also occurred in the four reactors. Nitrate assimilation accounted for 3.78%, 23.43%, 30.30%, and 43.78%, respectively, of the TN removal efficiencies with increased aeration intensity, as revealed by nitrogen-balance analysis (Fig. S2). No significant difference was found in COD degradation efficiencies amongst different aeration intensities ( $F = 4.42$ ,  $P_{0.05} = 0.066$ ; Table S3). This finding indicated that the aerobic metabolism of sodium succinate, as a readily biodegradable carbon source, may have depended on the presence of oxygen but did not increase with increased oxygen concentration. However, with further increased aeration intensity, TN removal rate did not increase and instead decreased, especially in R4 which did not achieve complete TN removal within 2 h. Similar results have been previously reported (Deng et al., 2020a, 2020b; John et al., 2020), i.e., TN removal efficiency initially increases and then decreases with increased aeration intensity. Combined analysis with the distribution patterns of COD (Fig. 2b) revealed that the imbalance between the reduction equivalent produced by the degradation of COD and the oxidation equivalent introduced by the higher aeration intensity was the main reason for this phenomenon. The activity of some related enzymes sensitive to oxygen could be another potential reason. To further explore the possible N-conversion pathway in denitrification, the accumulation of  $\text{NO}_2^-$  was analyzed (Fig. 2d), and results showed that nitrite concentration initially increased to the peak first and then decreased rapidly during the initial 10–50 min. This finding indicated typical partial denitrification supported by the endogenous electron donor as reported by Du et al. (2019). The apexes of nitrite accumulation in each system was not the same, and the maximum was 24 mg/L achieved in R1 without aeration. No key enzymes involved in anoxic denitrification were inhibited, so the accumulation of nitrite in the R1 case may be due to the use of polyhydroxyalkanotes stored in the non-denitrification stage as endogenous carbon sources. However, similar to the case of  $\text{NO}_3^-$  and TN, when aeration was 1.25 L/(L·min),  $\text{NO}_2^-$  accumulation occurred and complete removal was not achieved. Thus, different from anoxic denitrification (R1), whether the removal patterns of TN and nitrate and the accumulation of nitrite in R2, R3, and R4 (especially in R4) were caused by the competition amongst electron donors or enzyme inhibition required further study.

### 3.1.3. Analysis of denitrification efficiency under different aeration intensities based on NADH content distribution

As described by Chen and Strous (2013), in the respiratory chain of denitrification or oxygen respiration, electrons were all transferred from NADH to the reductase of the corresponding electron receptor, such as nitrate reductases or terminal oxidases, to contribute to proton

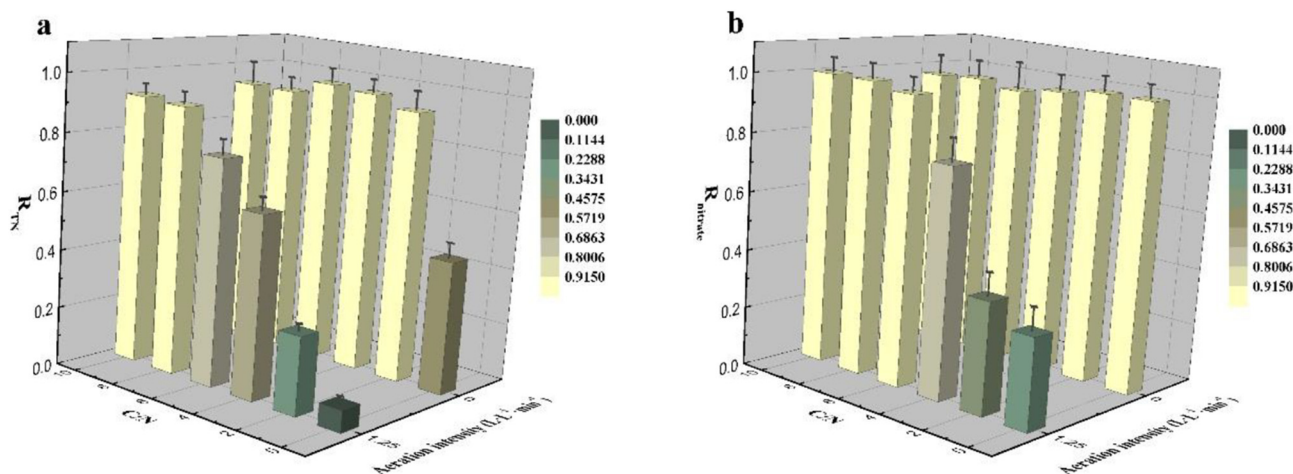


Fig. 1. Denitrification performance under different aeration intensities and C/N ratios. (a) Removal efficiency of TN ( $R_{TN}$ ), (b) Removal efficiency of nitrate ( $R_{nitrate}$ ).

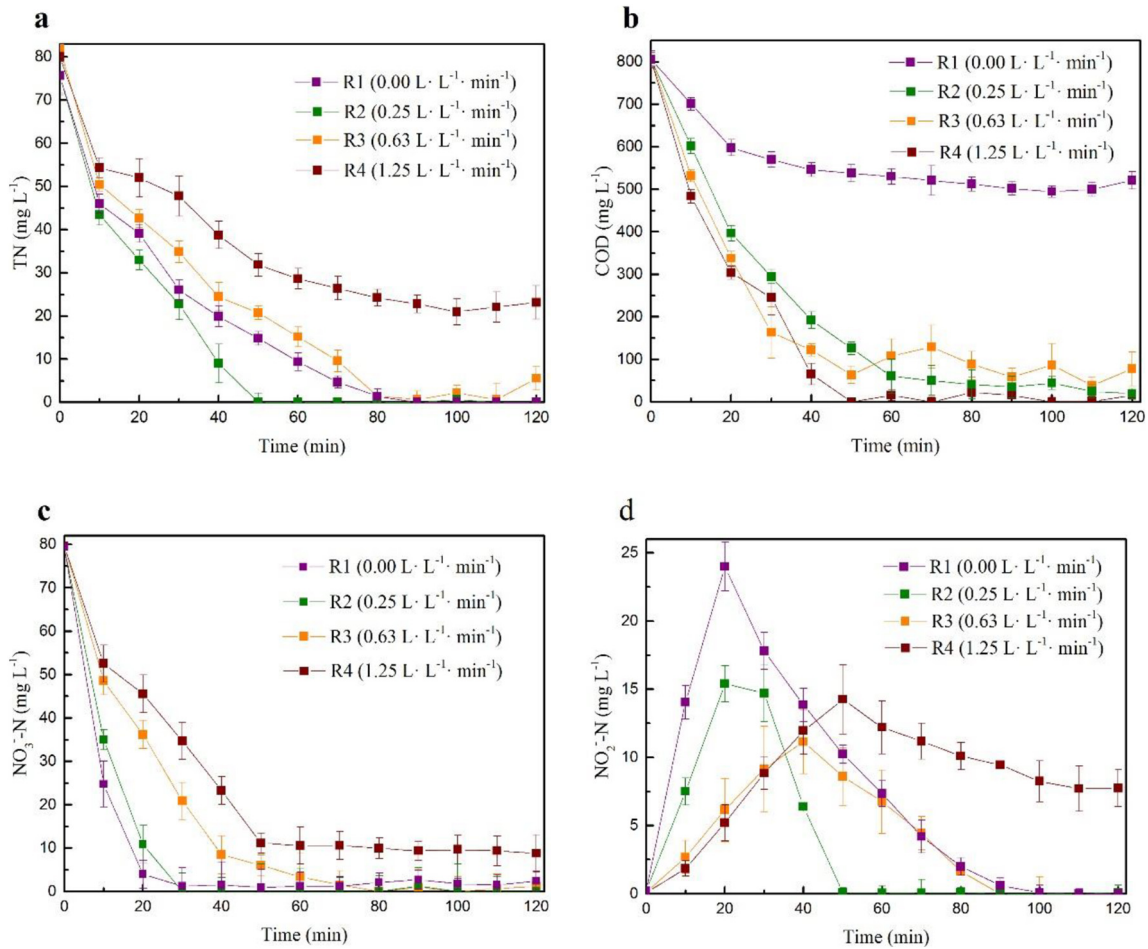


Fig. 2. The distribution patterns of intermediates under different aeration intensities. (a) TN, (b) COD, (c) NO<sub>3</sub><sup>-</sup> and (d) NO<sub>2</sub><sup>-</sup>.

translocation. Accordingly, the distribution of NADH in different aeration intensities was analyzed. As shown in Fig. 3, the intracellular NADH in R3 and R4 were significantly lower than those in R1 and R2, which may be due to the fact that the electron acceptor (e.g., O<sub>2</sub>) in the high aeration system was significantly higher than that in the low aeration system. As shown in Fig. S3, we detected DO values of 0.06–0.51, 0.17–4.14, 0.65–4.46, and 1.38–4.58 mg/L in R1, R2, R3, and R4 respectively, which did not linearly varying with aeration intensity (Deng et al., 2020a, 2020b; John et al., 2020). Furthermore, the increase in oxygen concentration can strengthen the assimilation and dissimilation of organic carbon which can also potentially influence denitrification efficiency by affecting NADH synthesis (Deng et al., 2020a, 2020b). As a result, the intracellular NADH slowly increased in the aeration systems, and the accumulation rates of NADH were 0.061, 0.016, and 0.013 ng/(mg Pro·min) in R2, R3, and R4, respectively. Correspondingly, as shown in Table 1, the TN removal rate under R2, R3, and R4 aeration rates were 1.45, 0.86, and 0.53 mg/(L·min), respectively. We found that under aeration conditions, the content and accumulation

rate of NADH were positively correlated with TN removal efficiency, i.e., more electron donors meant higher N transformation efficiencies. Theoretically, as a direct reduction equivalent produced by COD degradation, the accumulation of NADH was positively correlated to COD degradation efficiency. However, the relationships between COD degradation rate and NADH accumulation rate under different aeration intensities indicated that the introduction of oxygen can promote the production and consumption of NADH simultaneously. The consumption of NADH may have exceeded its production when aeration intensity surpassed a

Table 1  
Production and removal rate of NADH, TN, COD and NO<sub>3</sub><sup>-</sup> under different aeration intensities.

	R1	R2	R3	R4
NADH	-0.026	0.061	0.016	0.013
TN	-0.93	-1.45	-0.86	-0.53
COD	-4.31	-12.11	-14.61	-15.76
NO <sub>3</sub> <sup>-</sup>	-3.77	-3.43	-1.71	-1.31

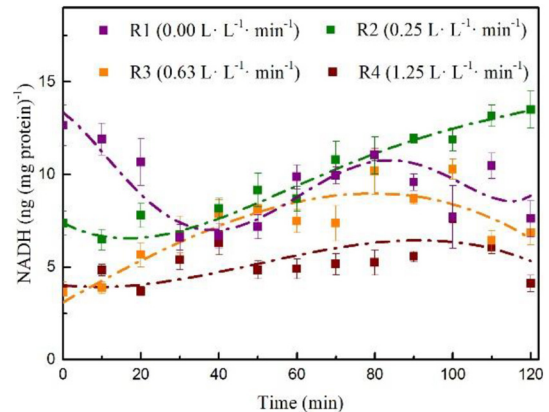


Fig. 3. Variations in intracellular NADH content under different aeration intensities.

certain threshold. Systematically, the introduction of oxygen promoted the degradation of organic carbon and the formation of NADH to a certain extent, but the amount of oxygen as an electron acceptor also increased, thereby increasing the consumption of NADH and competing with  $\text{NO}_3^-$  for electrons. Consequently, TN removal efficiency decreased, meaning that appropriate aeration intensity can enable the efficient removal of COD whilst stimulating TN removal without NADH being consumed by extra-oxygen.

### 3.1.4. Expression of heterotrophic denitrifying key genes under different aeration intensities

To adapt to different growth micro-environments, bacteria implement different metabolic processes through optimal enzyme expression to match the stable and efficient operation of related systems (Deng et al., 2020a, 2020b). As shown in Fig. 4, the relative expression of *napA*, *nirK*, and *nosZ*, a series of HD key genes, were all the highest in R2, consistent with the highest TN/ $\text{NO}_3^-$  removal efficiency as mentioned in Fig. 2. The activity of *napA* was less inhibited by oxygen and can be expressed preferentially, which was vital for the aerobic denitrification, and *napA* gene can be the proof of aerobic denitrification (Zhou et al., 2019). *nirK* and *nirS* can catalyze the second step of denitrification by expressing copper-type and cytochrome *cd1*-containing nitrite reductase under aerobic or anaerobic conditions. *nosZ* is the key gene catalyzing  $\text{N}_2\text{O}$  reduction to  $\text{N}_2$ . Many studies have shown that the expression of *nosZ* gene is inhibited by  $\text{O}_2$  to some extent in many genera compared with other denitrifying genes (e.g., *nirS*, *nirK*, and *napA*), which can lead to increased  $\text{N}_2\text{O}$  formation (Hu et al., 2015). However, similar to this experiment, Park et al. (2017) showed significant  $\text{N}_2\text{O}$  removal when  $\text{O}_2$  is initially present. He found that the transient presence

of  $\text{O}_2$  can promote  $\text{N}_2\text{O}$  reduction by strain T-27, whose  $\text{N}_2\text{O}$  reduction activity can be resuscitated by spiking the culture with  $\text{O}_2$ . Moreover, the abundance increment of these two kinds of denitrification genes (*nir* + 0.97% and *nos* + 0.6%) was obtained when low DO (0.5 mg/L) was applied in a continuous nitrogen removal process (Jiang et al., 2019). Interestingly, the relative abundance of genes involved in denitrification in this experiment neither inhibited nor increased with increased aeration intensity. We hypothesized that this finding was due to the increased electron flux flowing to  $\text{O}_2$  with increased aeration intensity. The mass-balance analysis of electron donor and acceptor showed that with increased aeration intensity, the flux of electrons to oxygen increased, which thermodynamically promoted the carbon-related metabolic process (S5). Higher aeration intensity meant greater promoting effect on aerobic respiration, which showed that the introduction of oxygen promoted the metabolism, proliferation, energy production, and conversion process of microorganisms. Furthermore, *narG* (as the representative gene of anoxic reductase of nitrate) appeared in all denitrification systems, and its abundance had a significant negative correlation with aeration intensity. Thus, even in the aeration systems, the combination of aerobic and anoxic denitrification remained. The high abundance of *napA* and *narG* in R2 further indicated that the synergistic effect of aerobic and anoxic denitrification explained the higher TN removal efficiency of this system.

### 3.2. Microbial community composition under different aeration intensities

#### 3.2.1. Reliability analysis of the high sequencing data

Rarefaction and rank-abundance curves were wide and flat (S7), indicating that the amount of sequencing data was reasonable and that

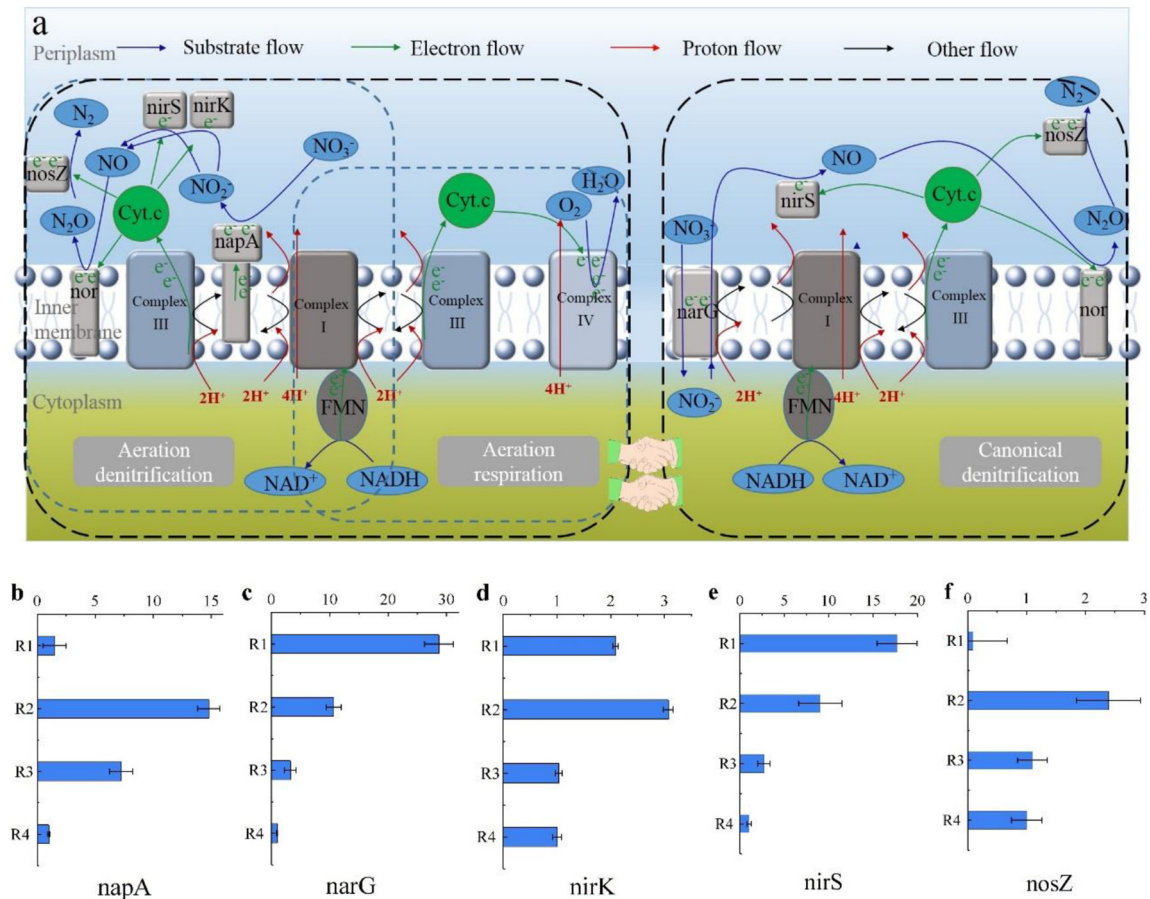


Fig. 4. Responses of heterotrophic denitrification enzyme activity. (a) Schematic diagram of electron transport system in aeration denitrification and canonical anoxic denitrification; (b-f) Relative abundance of key denitrifying gene.

the MiSeq high-throughput sequencing of 16S provided sufficient accurate information to study the diversity and structure of the microbial community.

### 3.2.2. Diversity-index analysis of bacterial communities

The Shannon and Simpson indices are often used to quantitatively describe the biodiversity of a system. A larger Shannon value or a smaller Simpson value meant greater community diversity. Table 2 showed that in R1, R2, R3, and R4, the Shannon indices were 2.98, 3.15, 3.18, and 3.29, respectively, and the Simpson indices were 0.16, 0.12, 0.11, and 0.09, respectively. Thus, with increased aeration intensity, the system biodiversity also increased. These results also verified previous descriptions that the performance of a bioreactor is positively correlated with the abundance of keystone taxa (e.g., functional bacteria) rather than the overall community diversity (Banerjee et al., 2018).

### 3.2.3. Analysis of microbial community structure under different aeration intensities

The microbial taxonomic distributions of the different denitrification systems were analyzed at the phylum (Fig. 5a) and genus (Fig. 5b) levels. Relative abundance varied depending on the aeration intensity at both these levels. Proteobacteria was dominant at the phylum level, and its relative abundances in R1, R2, R3, and R4 were 56.89%, 69.35%, 71.85%, and 51.51%, respectively. However, Firmicutes (18.04%), Bacteroidetes (8.17%), Chloroflexi (6.46%), and Synergistetes (8.55%) were enriched in R4 and were seldom or not found in each of the aeration system (R2–R4). Additionally, as the only phylum found only in aeration systems, the abundance of Verrucomicrobia gradually increased with increased aeration intensity, proving that the enhancement in aerobic metabolism of OHB could co-exist with Proteobacteria affiliated denitrifying bacteria under high-aeration-intensity conditions. To further determine which genera were responsible for nitrogen removal and the distinction amongst the different aeration intensities, the OTUs classified to genus level were analyzed. Phylum Proteobacteria was primarily dominated by genus *Propionivibrio* (36.25%), *Azoarcus* (22.68%), *Azoarcus* (27.21%), and *Paracoccus* (16.48) in R1, R2, R3, and R4, respectively. An obvious difference in microbial structure was found between the aeration and non-aeration systems, consistent with that at the phylum level. However, in the non-aeration system, the dominant genus involved in denitrification was *Propionivibrio*, which also belong to Proteobacteria, *Propionivibrio* (Liu et al., 2017; Thrash et al., 2010) (36.25%), *Cloacibacillus* (Ganesan et al., 2008) (7.23%), and *Ornatilinea* (Podosokorskaya et al., 2013) (5.87%) are anaerobic bacterium. However, *Paracoccus* (Watsuntorn et al., 2020) (7.97%), *Thauera* (Yang et al., 2019) (4.39%), and *Stappia* (Biebl et al., 2007) (2.13%) are facultative aerobic bacteria (FAB). Meanwhile, the aeration system primarily consisted of aerobic or facultative aerobic denitrifying bacteria. As shown in Fig. 5b, *Azoarcus* (Lee et al., 2014), *Paracoccus*, *Propionivibrio*, *Thauera*, *Stappia*, and *Pseudomonas* were the major genera accounting for 46.89% of all assigned OTUs in the four denitrification systems, and they are important denitrifying microorganisms.

NMDS analysis (S8) revealed that the samples from these reactors differed significantly, indicating that aeration intensity significantly influenced the denitrification microbial community structure. The total abundance of denitrification-affiliated core bacteria in R1, R2, R3, and

R4 were 51.87% (*Propionivibrio*, *Paracoccus*, *Thauera*, *Stappia*, *Pseudomonas*, and *Azoarcus*), 53.68% (*Azoarcus*, *Paracoccus*, *Thauera*, *Stappia*, and *Pseudomonas*), 51.28% (*Azoarcus*, *Paracoccus*, *Thauera*, *Pseudomonas*, and *Stappia*), and 32.34% (*Paracoccus*, *Stappia*, *Azoarcus*, *Thauera*, and *Pseudomonas*), respectively. As stated by Banerjee et al. (2018), keystone taxa performing the primary role in denitrification are highly related taxa and considerably impact the structure and function of the microbiome. Their abundance is negative correlated with aeration intensity (R2, R3, and R4) and peak in R2. According to these results, we speculated that superior performance can be achieved in a system with highly biodiverse communities having more keystone taxa. Based on this hypothesis, the resilient ability of R2 could be correlated with the co-occurrence network trait, where a shift in the state of a certain genus does not influence the variations in other genera nor destroy the niche any more (Deng et al., 2019). Furthermore, FAB were obtained in R1, R2, R3, and R4, especially in R2. These bacteria were *Azoarcus*, *Paracoccus*, *Thauera*, *Stappia*, and *Pseudomonas*, which were domesticated by the insufficient electron donor.

### 3.3. Microbial metabolic characteristics and potential networks under different aeration intensities

#### 3.3.1. KEGG metabolic characteristic analysis based on PICRUSt

The microbial community structure in the denitrification system significantly differed between aeration and non-aeration conditions, but no significant difference existed in TN removal efficiency amongst R1, R2, and R3 ( $F = 1.545$ ,  $P_{0.05} = 0.288$ ). Accordingly, we deeply explored the influence of different aeration intensities on denitrification based on the analysis of metabolic characteristics. Based on the analysis of the genetic function of existing sequencing microbial genomes, we quantitatively analyzed the functional differences amongst different samples. Fig. 6a shows that microorganisms in different aeration systems had divergences in functional-gene abundance, in which the abundances of membrane transport, amino acid metabolism, carbohydrate metabolism, and energy metabolism all increased with increased aeration intensity. Amino acid metabolism in the process of sewage treatment refers to a series of processes in which the protein in sewage undergoes the action of ammoniated bacteria and finally decomposes into ammonia nitrogen. On one hand, this finding indicated that the available carbon source in the system was reduced, and that the system entered the famine stage. On the other hand, because no protein was present in the influent and no significant difference existed in the TN removal efficiency amongst R1, R2, and R3 ( $F = 1.545$ ,  $P_{0.05} = 0.288$ ), the microbial community may have adapted to the environment by strengthening the amino acid metabolism to maintain its function. During starvation, amino acid metabolites are used as nutrients for the growth of heterotrophs (Chloroflexi, whose abundance increases with increased aeration intensity) or by participating in protein synthesis in EPS to achieve sludge granulation, i.e., a self-protection mechanism in the period of environmental deterioration (Sun Y. et al., 2019). With increased aeration intensity, a slight increase in nitrate in the effluent (Fig. 2c) and the presence of *Nitrospirae* in the aerobic denitrification system were observed, indicating the production of ammonia from amino acids metabolism which could be used by nitrifiers. Lawson et al. (2017) also found that the oxidation of amino acids coupled with the reduction of nitrate to nitrite by the heterotrophic denitrifiers can consolidate the overall nitrogen removal in natural ecosystem. In summary, we proved from the perspective of microbial metabolic characteristics that higher aeration intensity enhanced the microbial metabolic activity and mutual collaboration of different denitrification systems to adapt to a dynamic environment and form a self-protection mechanism for function maintenance.

#### 3.3.2. Potential network analysis based on SparCC

In ecology, functionally closely related communities are often considered to show the “same ascent and descent” in abundance and are

**Table 2**  
Diversity indices analysis of the four activated sludge samples.

Sample ID	OUT num	Shannon index	ACE index	Chao index	Simpson index
R4	2403	3.29	38,688.16	14,569.7	0.09
R3	1938	3.18	32,773.55	13,005.14	0.11
R2	2152	3.15	35,379.37	13,458.25	0.12
R1	1977	2.98	24,383.11	11,566.17	0.16

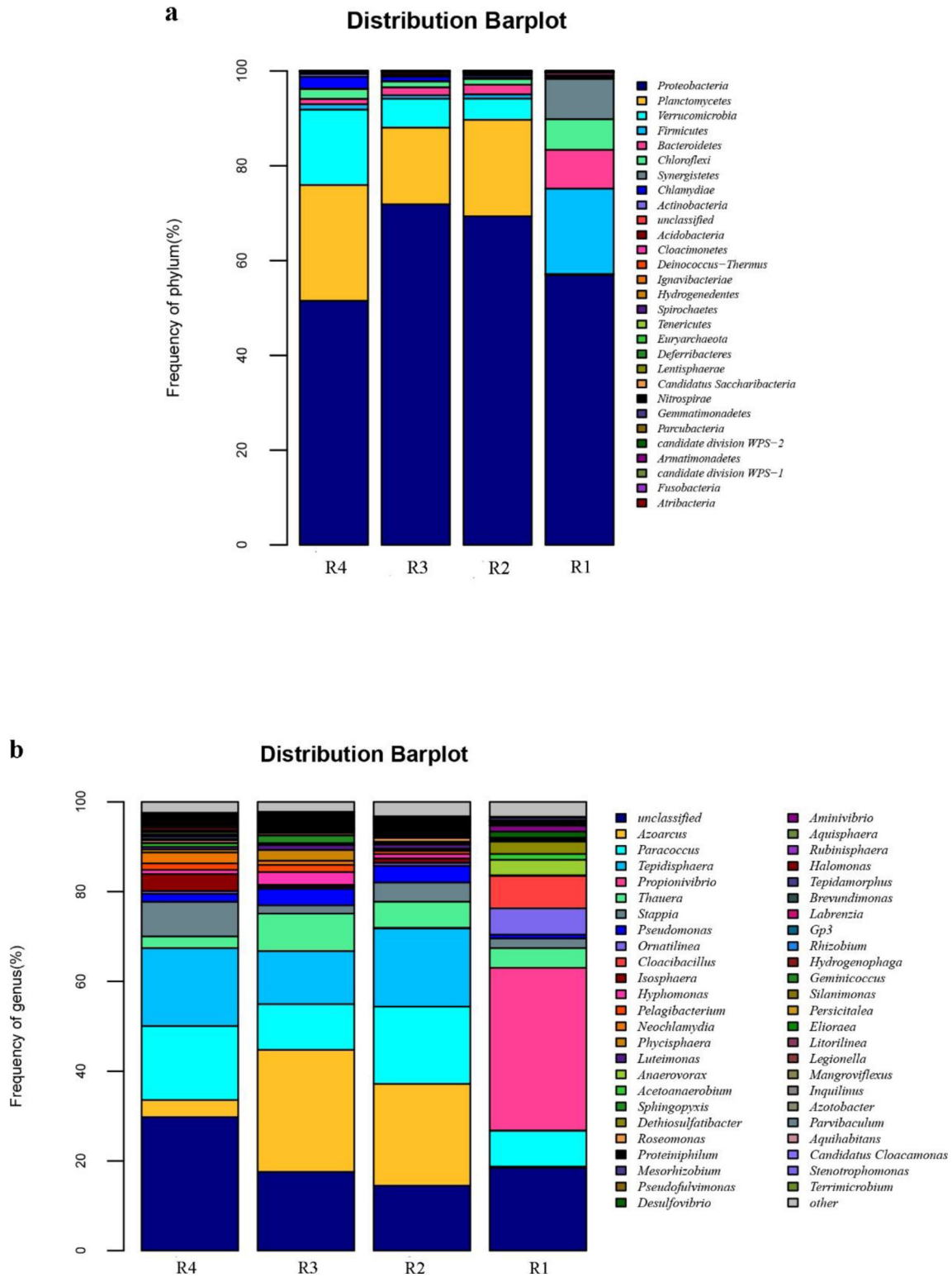
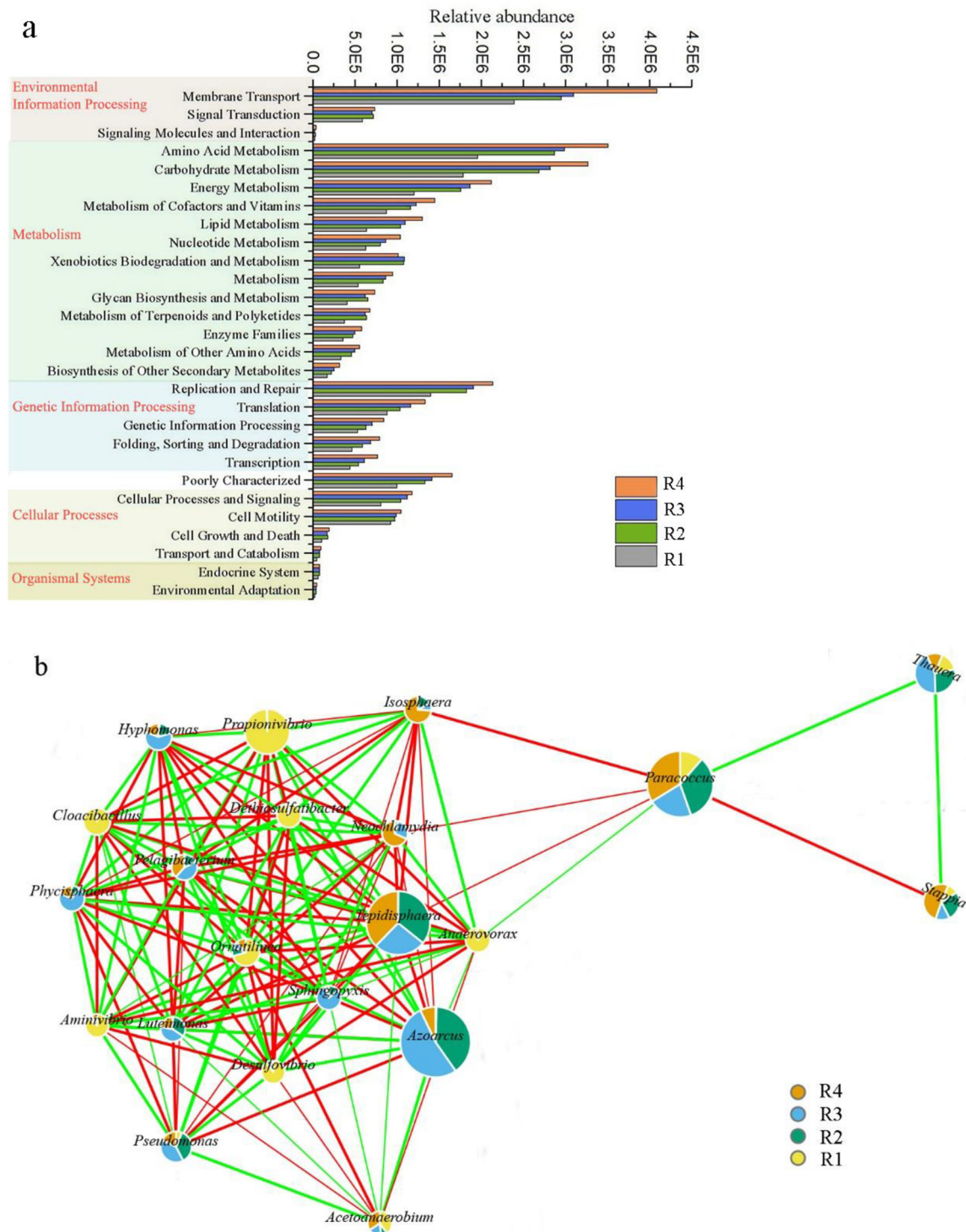


Fig. 5. Relative abundance of the dominant bacteria. (a) phylum level; (b) genus level.

divided into different co-abundance groups. Consequently, potential bacterial network interactions occur. Thus, the interactions of denitrifiers with other denitrifiers or OHB in an aerobic denitrification system and the effects of interactions on system performance with increased aeration intensity require further clarification. Remarkably, genes *Azoarcus* achieved the first highest abundance in R2 and R3 and achieved the fifth highest abundance in R4. As depicted in Fig. 6b,

*Pseudomonas* was the dominant denitrifiers that had a positive correlation with *Azoarcus* at the genus level, suggesting that these two organisms consistently interacted with one another in aerobic denitrification systems. In canonical sewage-treatment plants, *Azoarcus* and *Pseudomonas* are often associated with denitrification as heterotrophic denitrifiers. Based on metagenome analysis, Sun C. et al. (2019) found that denitrifiers of *Azoarcus* and *Pseudomonas* within Proteobacteria have DCG genes, a



**Fig. 6.** Microbial metabolic characteristics (a) and Co-occurrence potential network (b) of the four denitrification systems under different aeration intensities. The nodes in b represents different genus, and the different color blocks in the nodes represent the abundance of different samples in the genus classification. Red lines indicate positive interactions, and green lines indicate negative interactions. When the correlation coefficient is greater than 0.8, it is indicated by a thick line, and the thicker the line, the stronger the correlation.

quorum-sensing system which could boost microorganisms' cooperation with one another and eventually achieve nitrogen removal. He also found that the quorum-sensing system can promote bacterial aggregation by regulating EPS production under unfavourable conditions (e.g., famine). In contrast to syntrophy in R1, Betaproteobacteria affiliated denitrifying bacteria in R2–R4 (i.e., *Azoarcus*, *Paracoccus*, *Thauera*, *Stappia*, and *Pseudomonas*) may share symbiotic relationships which are based on

metabolism to realize TN removal and based on protection against chemical or mechanical pressure (Morris et al., 2013). Notably, *Azoarcus* and *Tepidisphaera* also showed a positive correlation. Some studies have demonstrated that *Azoarcus*, as a FAB, can couple with *Tepidisphaera* which can grow with the production of acetate and exopolysaccharides and achieve the removal of sulfide and nitrate by using acetate as an electron donor (Zhang et al., 2018). *Tepidisphaera*, belonging to phylum

Planctomycetes, is a newly described genus comprising moderately thermophilic, facultative aerobic cocci and occur as single cells or shapeless aggregates at the optimum temperatures of 47–50 °C and pH values of 7.0–7.5 (Kovaleva et al., 2015). *Tepidisphaera* reportedly degrade mono-, di-, and polysaccharides and also produce exopolysaccharides, acetate, propionate, and amino acid in liquid environments but cannot use nitrate and nitrite as an electron acceptor (Kovaleva et al., 2015). The co-occurrence between *Azoarcus* and the polysaccharide-hydrolyzing bacterium *Tepidisphaera* is a typical instance of commensalism, i.e., the former cross-feeds on substrate produced by the latter (Morris et al., 2013). *Azoarcus* also showed a significant positive correlation with *Hyphomonas*, *Pelagibacterium*, and *Sphingopyxis*. They all belong to *Proteobacteria*, which are oval or rod-shaped aerobic or facultative gram-negative bacteria. Research has shown that although part of *Hyphomonas* can reduce nitrate, none of them can conduct complete denitrification (Li et al., 2014; Li et al., 2016). Meanwhile, only part of *Pelagibacterium* (Yang and Sun, 2016) and *Sphingopyxis* species (Chen et al., 2018) can realize nitrate reduction. Some researchers also believe that *Sphingopyxis* is a strict aerobe that can grow anaerobically using nitrate as a terminal electron acceptor, which may confer an environmental advantage to itself (García-Romero et al., 2016). Thus, the synergistic effect amongst microorganisms in an aerobic denitrification system was primarily reflected in two aspects: intra-phylum cooperation amongst denitrifiers to achieve complete nitrogen removal, and inter-phylum cooperation amongst heterotrophs to build the best habitat and adapt to environmental changes. The findings were different for R1. *Propionivibrio* (anaerobe) and *Paracoccus* (facultative aerobe) were the dominant genera and showed a significant negative correlation (Fig. 6b). *Paracoccus* can use oxygen and nitrate as electron acceptors and can achieve higher denitrification efficiency for nitrate under aerobic than under completely anaerobic conditions (Watsuntorn et al., 2020). Accordingly, the presence of *Paracoccus* created an anaerobic micro-environment for the denitrification of *Propionivibrio* by competing for substrate and consuming oxygen simultaneously. The negative correlation of the two may have facilitated the complete removal of TN under different DO conditions, which was also inter-genus cooperation. Meanwhile, intra-genus cooperation occurred within *Propionivibrio* (*P. dicarboxylicus*, *P. limicola*, *P. pelophilus*, and *P. militaris*) (Li et al., 2019; Liu et al., 2017; Thrash et al., 2010), in which *P. dicarboxylicus*, *P. pelophilus*, and *P. limicola* were fermentative bacterium and can utilize succinate with propionate and acetate as major products. Meanwhile, *P. militaris* which is a non-fermentative, facultative anaerobe can completely oxidize propionate and acetate with oxygen, nitrate, and nitrite as electron acceptors to realize complete TN removal. This thermodynamic dependence amongst anaerobic microorganisms, in which the products of fermentation can be utilized as substrates by non-fermentative organisms to eliminate substrate inhibition, is known as syntrophy (a type of mutualism).

Creatively interpreting taxa in genus–genus association network interactions such as syntrophy, competitive interactions, and symbiotic relationships can enable the microbial ecology of different HD systems to form a plain description of community structure and a set of keystone taxa with potential microbial interactions regulated by aeration intensity. The aeration strategy as an ecological factor could be directly applied to guide the system towards optimal performance.

#### 4. Conclusions

The influence of different aeration intensities on heterotrophic denitrification was studied systematically. The removal rates of TN under different aeration intensities of 0.00, 0.25, 0.63, and 1.25 L/(L·min) were 0.93, 1.45, 0.86, and 0.53 mg/(L·min), respectively, which were much higher than previously reported values for pure bacteria. The optimal aeration intensity was 0.25 L/(L·min), and under this condition, the maximum accumulation and accumulation rate of NADH was achieved. Furthermore, the relative expression of *napA*, *nirK*, and *nosZ* were all the highest under this condition. Assimilatory nitrate removal

accounted for 3.78%, 23.43%, 30.30%, and 43.78%, respectively, of the TN removal efficiencies with increased aeration intensity, as revealed by nitrogen-balance analysis. In the non-aeration reactor, *Propionivibrio* denitrifiers were the main participants in denitrification. However, the aeration system was primarily dominated by facultative autotrophic oxygen-tolerant denitrifiers, and the interaction mode amongst microorganisms also varied in different systems.

#### CRedit authorship contribution statement

**Haiguang Yuan:** Conceptualization, Methodology, Data curation, Writing – original draft. **Shaobin Huang:** Conceptualization, Supervision. **Jianqi Yuan:** Visualization, Investigation. **Yingying You:** Software. **Yongqing Zhang:** Writing – review & editing.

#### Declaration of competing interest

The authors declare that they have no known competing financial interests or personal relationships that could have appeared to influence the work reported in this paper.

#### Acknowledgements

This research is financially supported by the National Natural Science Foundation of China (No. U1701243), National Key R&D Program of China (No. 2019YFC0408605), Research Project of Guangzhou Municipal Science and Technology Bureau (No. 201903010035) and Key-Area Research and Development Program of Guangdong Province (No. 2019B110209002).

#### Appendix A. Supplementary data

Supplementary data to this article can be found online at <https://doi.org/10.1016/j.scitotenv.2020.141965>.

#### References

- Andersson, S., Dalhammar, G., Kuttuva Rajarao, G., 2011. Influence of microbial interactions and EPS/polysaccharide composition on nutrient removal activity in biofilms formed by strains found in wastewater treatment systems. *Microbiol. Res.* 166 (6), 449–457.
- APHA, 2005. *Standard Methods for the Examination of Water and Wastewater*. 21st Edition. American Public Health Association, Washington DC.
- Banerjee, S., Schlaeppi, K., van der Heijden, M., 2018. Keystone taxa as drivers of microbiome structure and functioning. *Nat. Rev. Microbiol.* 16 (9), 567–576.
- Biebl, H., Pukall, R., Lünsdorf, H., Schulz, S., Allgaier, M., Tindall, B.J., Wagner-Döbler, I., 2007. Description of *Labrenzia alexandrii* gen. nov., sp. nov., a novel alphaproteobacterium containing bacteriochlorophyll a, and a proposal for reclassification of *Stappia aggregata* as *Labrenzia aggregata* comb. nov., of *Stappia marina* as *Labrenzia marina* comb. nov. and of *Stappia alba* as *Labrenzia alba* comb. nov., and emended descriptions of the genera *Pannonibacter*, *Stappia* and *Roseibium*, and of the species *Roseibium denhamense* and *Roseibium hamelinense*. *Int. J. Syst. Evol. Microb.* 57 (5), 1095–1107.
- Chen, J., Strous, M., 2013. Denitrification and aerobic respiration, hybrid electron transport chains and co-evolution. *Biochimica et Biophysica Acta (BBA) - Bioenergetics* 1827 (2), 136–144.
- Chen, H., Piao, A.L., Tan, X., Nogi, Y., Yeo, J., Lu, H., Feng, Q.Q., Lv, J., 2018. *Sphingorhabdus buctiana* sp. nov., isolated from fresh water, and reclassification of *Sphingopyxis contaminans* as *Sphingorhabdus contaminans* comb. nov. *Antonie Van Leeuwenhoek* 111 (3), 323–331.
- Chen, S., Li, S., Huang, T., Yang, S., Liu, K., Ma, B., Shi, Y., Miao, Y., 2020. Nitrate reduction by *Paracoccus thiophilus* strain LSL 251 under aerobic condition: performance and intracellular central carbon flux pathways. *Bioresour. Technol.* 308, 123301.
- Deng, Y., Ruan, Y., Zhu, S., Guo, X., Han, Z., Ye, Z., Liu, G., Shi, M., 2017. The impact of DO and salinity on microbial community in poly(butylene succinate) denitrification reactors for recirculating aquaculture system wastewater treatment. *AMB Express* 7 (1).
- Deng, Y., Ruan, Y., Ma, B., Timmons, M.B., Lu, H., Xu, X., Zhao, H., Yin, X., 2019. Multi-omics analysis reveals niche and fitness differences in typical denitrification microbial aggregations. *Environ. Int.* 132, 105085.
- Deng, S., Peng, S., Xie, B., Yang, X., Sun, S., Yao, H., Li, D., 2020a. Influence characteristics and mechanism of organic carbon on denitrification, N<sub>2</sub>O emission and NO<sub>2</sub><sup>-</sup> accumulation in the iron [Fe(0)]-oxidizing supported autotrophic denitrification process. *Chem. Eng. J.* 393, 124736.
- Deng, S., Xie, B., Kong, Q., Peng, S., Wang, H., Hu, Z., Li, D., 2020b. An oxic/anoxic-integrated and Fe/C micro-electrolysis-mediated vertical constructed wetland for decentralized low-carbon greywater treatment. *Bioresour. Technol.* 315, 123802.

- Domingo-Félez, C., Mutlu, A.G., Jensen, M.M., Smets, B.F., 2014. Aeration strategies to mitigate nitrous oxide emissions from single-stage nitrification/anammox reactors. *Environ. Sci. Technol.* 48 (15), 8679–8687.
- Du, C., Cui, C., Qiu, S., Shi, S., Li, A., Ma, F., 2017. Nitrogen removal and microbial community shift in an aerobic denitrification reactor bioaugmented with a *Pseudomonas* strain for coal-based ethylene glycol industry wastewater treatment. *Environ. Sci. Pollut. R.* 24 (12), 11435–11445.
- Du, R., Peng, Y., Ji, J., Shi, L., Gao, R., Li, X., 2019. Partial denitrification providing nitrite: opportunities of extending application for anammox. *Environ. Int.* 131, 105001.
- Feng, L., Yang, J., Ma, F., Pi, S., Xing, L., Li, A., 2020. Characterisation of *Pseudomonas stutzeri* T13 for aerobic denitrification: stoichiometry and reaction kinetics. *Sci. Total Environ.* 717, 135181.
- Ganesan, A., Chaussonnerie, S., Tarrade, A., Dauga, C., Bouchez, T., Pelletier, E., Le Paslier, D., Sghir, A., 2008. *Cloacibacillus evryensis* gen. nov., sp. nov., a novel asaccharolytic, mesophilic, amino-acid-degrading bacterium within the phylum 'Synergistetes', isolated from an anaerobic sludge digester. *Int. J. Syst. Evol. Microb.* 58 (9), 2003–2012.
- Gao, H., Schreiber, F., Collins, G., Jensen, M.M., Svitlica, O., Kostka, J.E., Lavik, G., de Beer, D., Zhou, H.Y., Kuypers, M.M., 2010. Aerobic denitrification in permeable Wadden Sea sediments. *Isme J* 4 (3), 417–426.
- García-Romero, I., Pérez-Pulido, A.J., González-Flores, Y.E., Reyes-Ramírez, F., Santero, E., Floriano, B., 2016. Genomic analysis of the nitrate-respiring *Sphingopyxis granuli* (formerly *Sphingomonas macrogoltabida*) strain TFA. *BMC Genomics* 17 (1).
- Guimerà, X., Dorado, A.D., Bonsfills, A., Gabriel, G., Gabriel, D., Gamisans, X., 2016. Dynamic characterization of external and internal mass transport in heterotrophic biofilms from microsensors measurements. *Water Res.* 102, 551–560.
- Hu, H., Chen, D., He, J., 2015. Microbial regulation of terrestrial nitrous oxide formation: understanding the biological pathways for prediction of emission rates. *FEMS Microbiol. Rev.* 39 (5), 729–749.
- Huang, T., Guo, L., Zhang, H., Su, J., Wen, G., Zhang, K., 2015. Nitrogen-removal efficiency of a novel aerobic denitrifying bacterium, *Pseudomonas stutzeri* strain ZF31, isolated from a drinking-water reservoir. *Bioresour. Technol.* 196, 209–216.
- Ji, B., Yang, K., Zhu, L., Jiang, Y., Wang, H., Zhou, J., Zhang, H., 2015. Aerobic denitrification: a review of important advances of the last 30 years. *Biotechnol. Bioproc. E.* 20 (4), 643–651.
- Jia, Y., Zhou, M., Chen, Y., Luo, J., Hu, Y., 2019. Carbon selection for nitrogen degradation pathway by *Stenotrophomonas maltophilia*: based on the balances of nitrogen, carbon and electron. *Bioresour. Technol.* 294, 122114.
- Jiang, C., Xu, S., Wang, R., Feng, S., Zhou, S., Wu, S., Zeng, X., Wu, S., Bai, Z., Zhuang, G., Zhuang, X., 2019. Achieving efficient nitrogen removal from real sewage via nitrite pathway in a continuous nitrogen removal process by combining free nitrous acid sludge treatment and DO control. *Water Res.* 161, 590–600.
- John, Y., Langergraber, G., Adyel, T.M., Emery David, V., 2020. Aeration intensity simulation in a saturated vertical up-flow constructed wetland. *Sci. Total Environ.* 708, 134793.
- Kovaleva, O.L., Merkel, A.Y., Novikov, A.A., Baslerov, R.V., Toshchakov, S.V., Bonch-Osmolovskaya, E.A., 2015. *Tepidisphaera mucosa* gen. nov., sp. nov., a moderately thermophilic member of the class Phycisphaerae in the phylum Planctomycetes, and proposal of a new family, Tepidisphaeraceae fam. nov., and a new order, Tepidisphaerales ord. nov. *Int. J. Syst. Evol. Microb.* 65 (Pt 2), 549–555.
- Lawson, C.E., Wu, S., Bhattacharjee, A.S., Hamilton, J.J., McMahon, K.D., Goel, R., Noguera, D.R., 2017. Metabolic network analysis reveals microbial community interactions in anammox granules. *Nat. Commun.* 8, 15416.
- Lee, D., Wong, B., Adav, S.S., 2014. *Azoarcus taiwanensis* sp. nov., a denitrifying species isolated from a hot spring. *Appl. Microbiol. Biot.* 98 (3), 1301–1307.
- Leinweber, A., Fredrik Inglis, R., Kümmerli, R., 2017. Cheating fosters species co-existence in well-mixed bacterial communities. *The ISME Journal* 11 (5), 1179–1188.
- Li, A., Gai, Z., Cui, D., Ma, F., Yang, J., Zhang, X., Sun, Y., Ren, N., 2012. Genome sequence of a highly efficient aerobic denitrifying bacterium, *pseudomonas stutzeri* T13. *J. Bacteriol.* 194 (20), 5720.
- Li, C., Lai, Q., Li, G., Sun, F., Shao, Z., 2014. *Hyphomonas atlanticus* sp. nov., isolated from the Atlantic Ocean and emended description of the genus *Hyphomonas*. *Syst. Appl. Microbiol.* 37 (6), 423–428.
- Li, X., Li, C., Lai, Q., Li, G., Sun, F., Shao, Z., 2016. *Hyphomonas pacifica* sp. nov., isolated from deep sea of the Pacific Ocean. *Antonie Van Leeuwenhoek* 109 (8), 1111–1119.
- Li, C., Liu, S., Ma, T., Zheng, M., Ni, J., 2019. Simultaneous nitrification, denitrification and phosphorus removal in a sequencing batch reactor (SBR) under low temperature. *Chemosphere* 229, 132–141.
- Liu, C., Lin, S., Hameed, A., Liu, Y., Hsu, Y., Wong, W., Tseng, C., Lur, H., Young, C., 2017. *Oryzomicrobium terrae* gen. nov., sp. nov., of the family Rhodocyclaceae isolated from paddy soil. *Int. J. Syst. Evol. Microb.* 67 (2), 183–189.
- Luo, G., Li, L., Liu, Q., Xu, G., Tan, H., 2014. Effect of dissolved oxygen on heterotrophic denitrification using poly(butylene succinate) as the carbon source and biofilm carrier. *Bioresour. Technol.* 171, 152–158.
- Morris, B.E.L., Henneberger, R., Huber, H., Moissl-Eichinger, C., 2013. Microbial syntrophy: interaction for the common good. *FEMS Microbiol. Rev.* 37 (3), 384–406.
- Oh, J., Silverstein, J., 1999. Oxygen inhibition of activated sludge denitrification. *Water Res.* 33 (8), 1925–1937.
- Orellana, L.H., Chee-Sanford, J.C., Sanford, R.A., Löffler, F.E., Konstantinidis, K.T., 2018. Year-round shotgun Metagenomes reveal stable microbial communities in agricultural soils and novel Ammonia oxidizers responding to fertilization. *Appl. Environ. Microb.* 84 (2).
- Park, D., Kim, H., Yoon, S., 2017. Nitrous oxide reduction by an obligate aerobic bacterium, *Gemmatimonas aurantiaca* strain T-27. *Appl. Environ. Microbiol.* 83 (12).
- Peng, S., Deng, S., Li, D., Xie, B., Yang, X., Lai, C., Sun, S., Yao, H., 2020. Iron-carbon galvanic cells strengthened anaerobic/anoxic/oxic process (Fe/C-A2O) for high-nitrogen/phosphorus and low-carbon sewage treatment. *Sci. Total Environ.* 722, 137657.
- Podosokorskaya, O.A., Bonch-Osmolovskaya, E.A., Novikov, A.A., Kolganova, T.V., Kublanov, I.V., 2013. *Ornatilinea apprima* gen. nov., sp. nov., a cellulolytic representative of the class Anaerolineae. *Int. J. Syst. Evol. Microb.* 63 (Pt\_1), 86–92.
- Robertson, L.A., Kuenen, J., 1984. Aerobic denitrification: a controversy revived. *Arch. Microbiol.* 139 (4), 351–354.
- Sun, Y., Guan, Y., Wang, H., Wu, G., 2019. Autotrophic nitrogen removal in combined nitrification and Anammox systems through intermittent aeration and possible microbial interactions by quorum sensing analysis. *Bioresour. Technol.* 272, 146–155.
- Sun, C., Yuan, J., Xu, H., Huang, S., Wen, X., Tong, N., Zhang, Y., 2019. Simultaneous removal of nitric oxide and sulfur dioxide in a biofilter under micro-oxygen thermophilic conditions: removal performance, competitive relationship and bacterial community structure. *Bioresour. Technol.* 290, 121768.
- Thrash, J.C., Pollock, J., Torok, T., Coates, J.D., 2010. Description of the novel perchlorate-reducing bacteria *Dechlorobacter hydrogenophilus* gen. nov., sp. nov. and *Propionivibrio militaris*, sp. nov. *Appl. Microbiol. Biot.* 86 (1), 335–343.
- Wan, R., Wang, L., Chen, Y., Zheng, X., Chew, J., Huang, H., 2019. Tetrabromobisphenol A (TBBPA) inhibits denitrification via regulating carbon metabolism to decrease electron donation and bacterial population. *Water Res.* 162, 190–199.
- Watsuntorn, W., Kojonna, T., Rene, E.R., Lens, P., Chulalaksananukul, W., 2020. Draft genome sequence and annotation of *paracoccus versutus* MAL 1HM19, a nitrate-reducing, sulfide-oxidizing bacterium. *Microbiol Resour Annuoc* 9 (10).
- Whiteley, M., Diggle, S.P., Greenberg, E.P., 2017. Progress in and promise of bacterial quorum sensing research. *Nature* 551 (7680), 313–320.
- Xu, H., Zhao, X., Huang, S., Li, H., Tong, N., Wen, X., Sun, C., Fazal, S., Zhang, Y., 2018. Evaluation of microbial p-chloroaniline degradation in bioelectrochemical reactors in the presence of easily-biodegrading cosubstrates: degradation efficiency and bacterial community structure. *Bioresour. Technol.* 270, 422–429.
- Yang, N., Sun, C., 2016. *Pelagibacterium lixinzhangensis* sp. nov., a novel member of the genus *pelagibacterium*. *Curr. Microbiol.* 72 (5), 551–556.
- Yang, N., Zhan, G., Li, D., Wang, X., He, X., Liu, H., 2019. Complete nitrogen removal and electricity production in *Thauera*-dominated air-cathode single chambered microbial fuel cell. *Chem. Eng. J.* 356, 506–515.
- Yang, J., Feng, L., Pi, S., Cui, D., Ma, F., Zhao, H., Li, A., 2020a. A critical review of aerobic denitrification: insights into the intracellular electron transfer. *Sci. Total Environ.* 731, 139080.
- Yang, Y., Pan, J., Zhou, Z., Wu, J., Liu, Y., Lin, J., Hong, Y., Li, X., Li, M., Gu, J., 2020b. Complex microbial nitrogen-cycling networks in three distinct anammox-inoculated wastewater treatment systems. *Water Res.* 168, 115142.
- Zhang, R., Xu, X., Chen, C., Xing, D., Shao, B., Liu, W., Wang, A., Lee, D., Ren, N., 2018. Interactions of functional bacteria and their contributions to the performance in integrated autotrophic and heterotrophic denitrification. *Water Res.* 143, 355–366.
- Zhang, H., Zhao, Z., Li, S., Chen, S., Huang, T., Li, N., Yang, S., Wang, Y., Kou, L., Zhang, X., 2019. Nitrogen removal by mix-cultured aerobic denitrifying bacteria isolated by ultrasound: performance, co-occurrence pattern and wastewater treatment. *Chem. Eng. J.* 372, 26–36.
- Zhou, S., Zhang, Y., Huang, T., Liu, Y., Fang, K., Zhang, C., 2019. Microbial aerobic denitrification dominates nitrogen losses from reservoir ecosystem in the spring of Zhouchun reservoir. *Sci. Total Environ.* 651, 998–1010.